Scientific Research Publishing

Open Journal of Geology, 2025, 15(5), 245-264
https://www.scirp.org/journal/ojg
ISSN Online: 2161-7589
ISSN Print: 2161-7570

Petrological Characteristics of the Gneissic Formations in the Kenema-Man Domain: Biankouma-Kouibli Sector (Cote d'Ivoire West African Craton)

Brice Roland Kouassi[1*], Kouadio David Koffi[2], Yao Honoré Koffi[1], Alain Nicaise Kouamelan[2]

[1]UFR-Biological Sciences, Geosciences Department, Peleforo Gon Coulibaly University, Korhogo, Côte d'Ivoire
[2]Laboratory of Geology, Mineral and Energy Resources/Training and Research Unit in Earth Sciences and Mineral Resources, Félix Houphouët-Boigny University, Abidjan, Côte d'Ivoire
Email: *drbrice.kouassi@gmail.com

How to cite this paper: Kouassi, B.R., Koffi, K.D., Koffi, Y.H. and Kouamelan, A.N. (2025) Petrological Characteristics of the Gneissic Formations in the Kenema-Man Domain: Biankouma-Kouibli Sector (Cote d'Ivoire West African Craton). *Open Journal of Geology*, **15**, 245-264.
https://doi.org/10.4236/ojg.2025.155012

Received: March 21, 2025
Accepted: May 12, 2025
Published: May 15, 2025

Abstract

The gneissic formations constitute one of the major formations observed within the Archean domain of Côte d'Ivoire. Located in the northwest of Côte d'Ivoire, the gneissic formations of the Biankouma and Kouibli sectors were the subject of this study. In order to determine the geochemical and petrographic characteristics as well as the geotectonic environment of these rocks, petrographic studies associated with geochemical analyses were carried out. The geology of this area includes mainly metamorphic formations such as granulitic gneiss, charnockites, pink granulites, charnockitic gneiss and migmatitic gneiss with biotite. The mineralogy of these formations is dominated by quartz and feldspars associated with either biotite or hypersthene. The geochemical data indicate that these formations are generally granodioritic and tonalitic in composition; they are TTG. They have an essentially calc-alkaline affinity (strongly potassic), however tholeic occurrences are observable. The formations in the Biankouma and Kouibli sectors are weakly metaluminous to peraluminous and poor in alumina (Al_2O_3 < 15%). Rare earth spectra show an enrichment in light rare earths and a depletion in heavy rare earths. A negative europium anomaly is also observed. This anomaly implies the presence of feldspar, notably plagioclase in the residual liquid. Multi-element diagrams normalized to the early mantle showed enrichment in LILEs and depletion in HFSE. Negative Ta and Nb anomalies were observed in each of the samples. These indicate that the studied formations originate from the partial melting of the crust. Trace element data, including rare earths, indicate that the formations studied are derived from the partial melting of a basic composition

rock containing garnet and hornblende. All samples have a composition of arc and collision granites and would be generated in a subduction zone.

Keywords

Archean, Metamorphism, TTG, Rare Earths, Geodynamics, Biankouma and Kouibli

1. Introduction

The Earth's crust is predominantly composed of Archean and Paleoproterozoic materials, with over 75% of the continental crust having differentiated from the mantle during this period [1]. However, recent studies suggest limited crustal evolution during the Hadean [2] [3]. The Archean domain of the West African Craton (COA) mainly consists of orthogneisses and charnockites, particularly within the Réguibat and Man Ridges. These high-grade metamorphic formations are often associated with intrusive magmatic rocks. The geothermal gradients during the Archean were higher than those of the Paleoproterozoic [4], making this era distinct in terms of petrology, tectonics, and mineralization. Petrologically, Archean terrains are characterized by TTG (tonalite-trondhjemite-granodiorite) suites and komatiites. While komatiites are associated with greenstone belts, TTGs dominate granito-gneissic complexes. TTG studies remain significant for determining rock protoliths [5]. Gneissic formations, among the oldest rocks [6], are widespread in the Archean domain of Côte d'Ivoire but also occur in the transition zone between Archean and Paleoproterozoic terrains. Tectonically, Archean terrains exhibit predominantly vertical structures [7]-[10]. The Kenema-Man domain hosts Banded Iron Formations (BIFs), indicating a previously reducing atmosphere. The disappearance of BIFs corresponds to increased atmospheric oxygen levels [11] [12]. Petrogeochemical, structural, and geochronological studies [13] have provided insights into the lithological composition, geochemical characteristics, and tectonic evolution of this domain. This study aims to further contribute by analyzing the petrographic and geochemical properties of the gneisses in the Biankouma-Kouibli sector and assessing their emplacement context.

2. Geological Setting

The study area is located in western Côte d'Ivoire, between longitudes 7˚ and 8˚ West and latitudes 8˚ and 8˚30' North (**Figure 1**). It lies approximately 700 km north of Abidjan and 40 km north of Man. It is bordered by Touba to the north, Man to the south, Danané to the west, and Séguéla to the east.

The West African Craton includes two principal Precambrian domains: the Réguibat Rise to the North and the Leo-Man Rise to the South [14] [15]. The Leo-Man Rise is composed by an Archean cratonic nucleus in the southwest, the so-

called Kéména-Man domain (KMD), surrounded by some Paleoproterozoic belts in the north and east forming the Baoulé-Mossi domain (**Figure 2**) [16]. Following this first stage of crustal growth, the craton was affected by two major metamorphic and magmatic events; the Leonian cycle at ca. 3.2 - 3.0 Ga [17] and the Liberian cycle at ca. 2.9 - 2.8 Ga [17] [18]. The Baoulé-Mossi domain is made up by an association of mainly low-grade Birimian (ca. 2.20 - 2.13 Ga) and Tarkwaian (ca. 2.10 - 2.09 Ga) sediments and plutono-volcanic rocks, which emplaced during a major juvenile crust-forming event, referred as the Eburnean orogeny, and dated between ca. 2250 and 1980 Ma [15] [19]-[21].

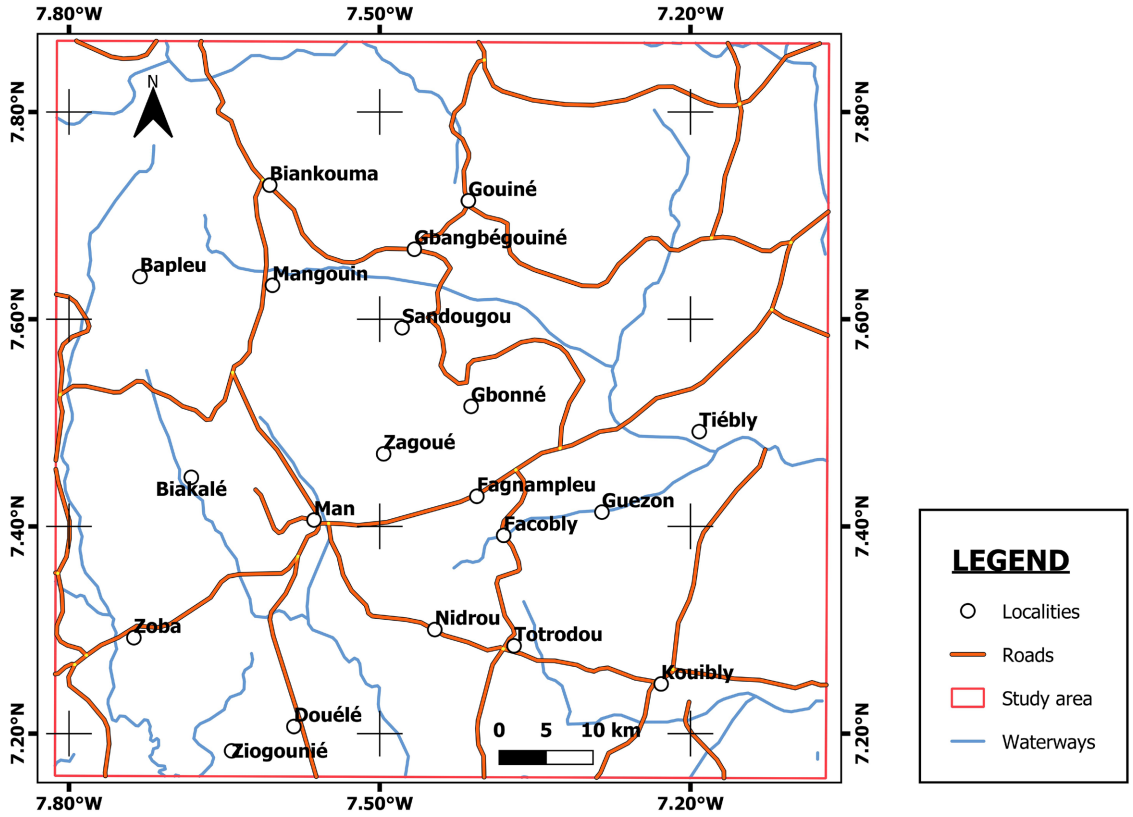

Figure 1. Location map of the study area.

Volcanic rocks geochemical signature is compatible with the evolution from tholeiitic oceanic crust or oceanic plateau to juvenile calc-alkaline volcanic island arcs [15].

The Baoule-Mossi Paleoproterozoic domain of the West African Craton (WAC) was accreted to the Archean nucleus of The WAC During the Eburnean orogeny [22]-[26] (**Figure 2**). The Baoule-Mossi domain is composed of Birimian greenstone belts made of metavolcanic, metavolcanosedimentary, and metasedimentary rocks, emplaced between 2220 and 2160 Ma [15] [27], And Bandamian Volcanic rocks aged between 2120 And 2080 Ma [24] [28] [29]. The study area is part of the Kenema-Man domain. The Archean domain or Kenema-Man domain is delimited by the Monts Trou fault trending SW-NE and the south-meridian Sas-

sandra fault up to the height of Odienné. It is located north of the Man-Danané fault. The region is governed mainly by gray granulitic gneisses, pink granulites, charnockites and some granitoids [30] (**Figure 3**).

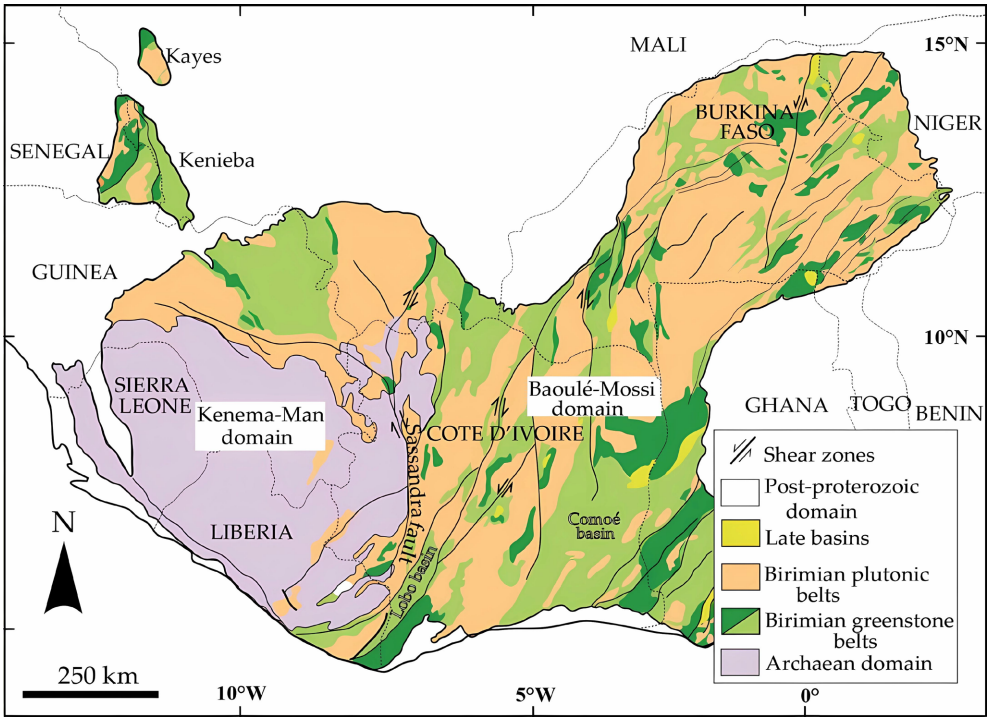

Figure 2. Simplified geological map of the West African craton (modified after the BRGM SIGAfrique map [16]

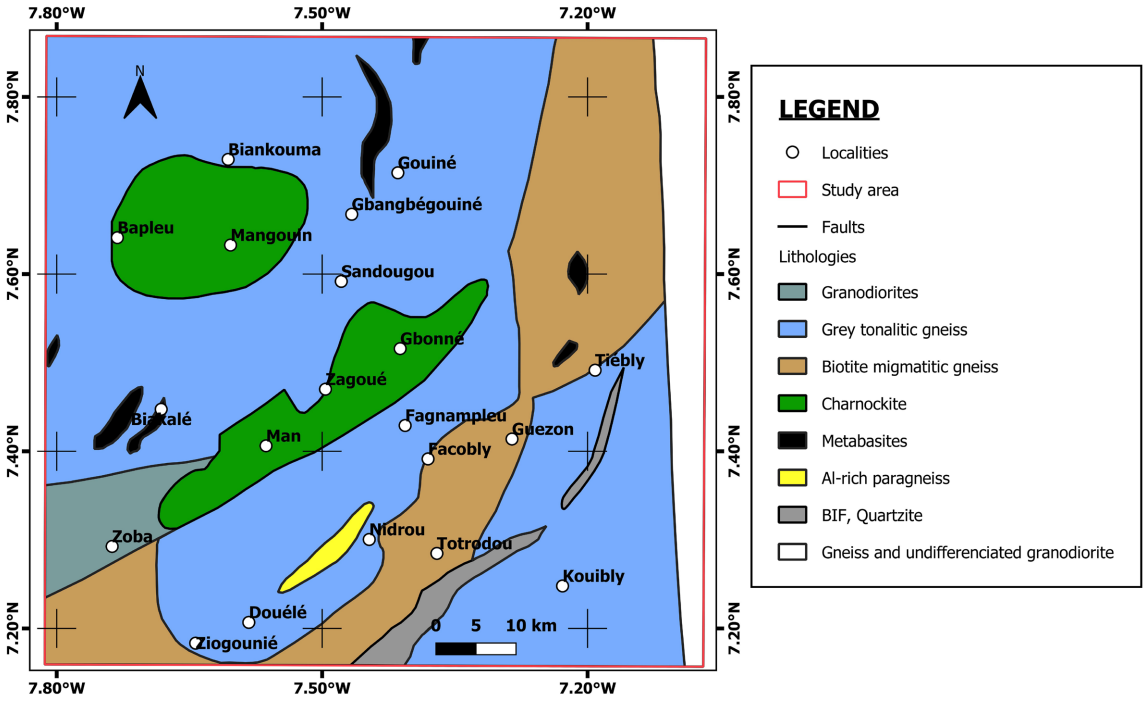

Figure 3. Geological map of the study area extracted from the 1/200,000 map of the Man domain according to [14].

These formations are intruded by pink granites, basic-ultrabasic complexes, granodiorites, and granites. Supracrustal rocks such as aluminous gneisses, amphibolo-pyroxenites, and ferruginous quartzites have undergone catazonal metamorphism during significant folding events [31]. Additionally, Birimian formations, including the Ity-Toulépleu unit (Danané region) and the layered mafic-ultramafic Yacouba complex (Biankouma-Sipilou region), have intruded the gneissic granulites of the Archean Man domain (3.6 - 2.78 Ga) [32].

3. Analytical Methods

3.1. Petrography

Table 1 contains all the samples submitted to this study. Macroscopic petrography was used to determine key rock characteristics, including texture, structure, color, degree of alteration, and mineralogical composition. To enhance the macroscopic analysis, eight thin sections were prepared at the Géoressources laboratory of the University of Lorraine for microscopic examination. These thin sections were analyzed using an Optika LD5500 polarizing optical microscope, providing insights into the primary and secondary mineral paragenesis, accessory mineral content, and textural relationships.

Table 1. Summary of the geographical coordinates of the samples studied.

Region	Locality	Samples	GPS Coordinates	
			Easting	Northing
MAN	Man-Biankouma axis	CIS 25	650034	834109
	Man-Biankouma axis	CIS 26	650500	838730
	Biankouma	CIS 27	652490	857092
		CIS 44	680751	805198
	Kouibli	CIS 45	685785	804202
		CIS 46	688892	803805

3.2. Geochemical Analyses of Whole Rocks

The bulk compositions of samples from various lithologies were determined using inductively coupled plasma optical emission spectrometry (ICP-OES) with an Icap 6500 spectrometer at CRPG (Nancy, France). Major and trace element analyses for silicates were conducted using an electron probe microanalyzer (EPMA) with a Cameca PC-controlled SX-100 (GeoRessources, Nancy). The analysis was performed with an accelerating voltage of 15 kV, a beam current of 12 nA, and a peak counting time of 10 to 20 seconds. The geochemical results, including major and trace element concentrations, are presented in Table 2 and Table 3.

Table 2. Major element composition of all our samples (% oxide weight).

Samples	CIS 25A	CIS 25B	CIS 26	CIS 27A	CIS 27B	CIS 44	CIS 45	CIS 46
SiO_2	73.2	73.4	70.5	68.6	72.9	59.16	74.6	70.15
Al_2O_3	13.5	14	14.2	14.8	13.4	16 .37	13.09	14.52

Continued

Fe_2O_3	2.7	1.8	3.7	4.4	2.4	8.6	2.51	3.25
CaO	1.5	1	2.7	2.4	1.3	5.8	2.94	1.92
MgO	0.4	0.2	0.9	0.9	0.3	2.41	1.27	0.63
Na_2O	3.7	3.5	3.4	4.1	3.2	5.04	3.57	3.25
K_2O	4	5.3	3.8	3.3	5.1	1.25	1.08	4.08
MnO	0	0.1	0.1	0.1	0	0.12	0.01	0.02
TiO_2	0.2	0.1	0.4	0.4	0.1	0.6	0.21	0.32
P_2O_5	0	0	0.1	0.1	0	0.15	0.01	0.1
Cr_2O_5	LD	LD	LD	LD	LD	LD	LD	LD
LOI	0.13	0.13	0.08	0.07	0.42	0.2	0.45	0.16
Total	99.24	99.31	99.57	99.02	98.69	99.5	99.29	99.02

Table 3. Trace element and rare earth composition (ppm) of all samples.

Samples	CIS 25A	CIS 25B	CIS 26	CIS 27A	CIS 27B	CIS 44	CIS 45	CIS 46
Ba	1796	1185	1451	1799	1680	259	385	1700
Be	<LD	<LD	<LD	<LD	<LD	<LD	<LD	<LD
Co	2.9	0.9	6.7	6.4	1.8	25.3	4.6	4.9
Cs	0.2	0.2	<LD	<LD	<LD	0 ;2	<LD	0 ;1
Ga	15.9	16.2	14.4	18.1	14	21.3	15.4	16.5
Hf	5.6	4	3.2	9.7	4.5	6.7	5.6	7.4
Nb	3.8	1.8	2.5	4.5	0.2	14.3	4.5	4.7
Rb	115.2	162.1	33.9	59.9	106.1	20.8	27.4	116.8
Sn	<LD	<LD	2	<LD	<LD	3	<LD	<LD
Sr	152.1	101.2	260.4	234.6	169.9	208.6	163.1	231.1
Ta	0.1	<LD	0.2	<LD	<LD	1.2	0.1	0.1
Th	59.7	6.7	0.9	43.5	46.5	2.7	9.5	42.7
U	2.4	1.3	0.1	1.6	3.1	6.5	0.1	1.1
V	10	<LD	40	26	<LD	97	13	18
W	<LD	<LD	<LD	<LD	<LD	<LD	<LD	<LD
Zr	193.1	118.8	148.6	402.8	152.6	261	205	292.5
Y	8.9	30.1	7.3	12.1	2.9	42.1	1.5	2.9
Mo	0.6	0.5	0.5	0.7	0.4	0.4	0.3	0.4
Cu	3.5	0.7	12.6	10	2.5	45.3	2.7	7.4
Pb	9.7	5.1	1.3	7.4	13.4	1.3	1.7	5.8
Zn	24	10	25	40	24	43	31	33
Ni	3.9	1.7	9.6	7.1	2.9	17.9	7.2	6.9
La	75.7	33.8	31.2	137.1	67.8	28.9	50.3	84.1
Ce	130.7	56.4	45.6	257.8	124	66.7	85.2	151.5
Pr	12.13	5.13	4.65	26.11	12.02	8.48	8.41	14.48

Continued

Nd	37.9	15.4	17.1	82.5	38.2	35.4	25	45.6
Sm	5.57	2.36	2.38	10.46	4.89	8.55	2.82	4.86
Eu	0.73	0.55	1.24	1.06	0.76	1.73	1.07	1.09
Gd	3.68	2.53	2.19	6.85	2.86	9.39	1.55	2.79
Th	0.4	0.51	0.26	0.66	0.23	1.36	0.11	0.22
Dy	1.89	4.38	1.41	3.1	0.83	8.48	0.43	0.79
Ho	0.34	0.99	0.26	0.42	0.08	1.55	0.03	0.09
Er	0.79	3.23	0.7	1.09	0.23	4.36	0.09	0.25
Tm	0.11	0.54	0.08	0.13	0.04	0.56	0.03	0.04
Yb	0.6	3.67	0.56	0.86	0.23	3.81	0.17	0.22
Lu	0.11	0.54	0.08	0.13	0.04	0.56	0.03	0.04

4. Lithology Results

4.1. Granulite Gneiss

Samples CIS 25A, CIS 27A, and CIS 27B, located north of the Man-Danané fault, consist of quartz-feldspathic formations with pyroxene. These massive rocks exhibit alternating light and dark bands. Under the microscope, they display a granoblastic structure, with quartz as the dominant mineral. Feldspar is mesoperthitic, while hypersthene appears rounded and undergoing alteration. The presence of hypersthene indicates a high degree of metamorphism. Brown biotite is rare, and opaque minerals constitute the majority of accessory phases (**Figure 4(A)**).

4.2. Charnockite

Charnockite (CIS 26) is a massive rock with no clear structural modifications, observed along the Man-Biankouma axis. The rock is grey-green with a porphyritic grainy texture and crystals exceeding 2 cm. It is a quartz-feldspathic rock with a granoblastic structure, containing a significant amount of plagioclase and orthopyroxene (hypersthene). Biotite is rare and forms due to pyroxene alteration. Opaque minerals and biotite dominate the accessory phases (**Figure 4(B)**).

4.3. Pink Granulite

Sample CIS 25B represents a pink granulite found north of the Man-Danané fault. This quartz-feldspathic rock exhibits a medium-grained granoblastic structure. Its mineral composition resembles granitoids, primarily consisting of quartz with rolling extinction, feldspar, and opaque minerals. The feldspar is strongly perthitic, giving it a zebra-like appearance (**Figure 4(C)**). The granulite facies is characterized by dark quartz.

4.4. Biotite Migmatitic Gneiss

Biotite migmatitic gneiss (CIS 44 and CIS 45) appears as a massive formation with

more pronounced foliation than the gray gneisses of the northern zone. This quartzo-feldspathic rock has a granoblastic structure, with feldspar (mainly plagioclase) exhibiting minimal perthitic texture. Quartz shows rolling extinction, while biotite appears in brown or green, crystallizing in an oriented manner that defines the foliation. The accessory phases include garnet, opaque minerals, and zircons associated with biotite (**Figure 4(D)**).

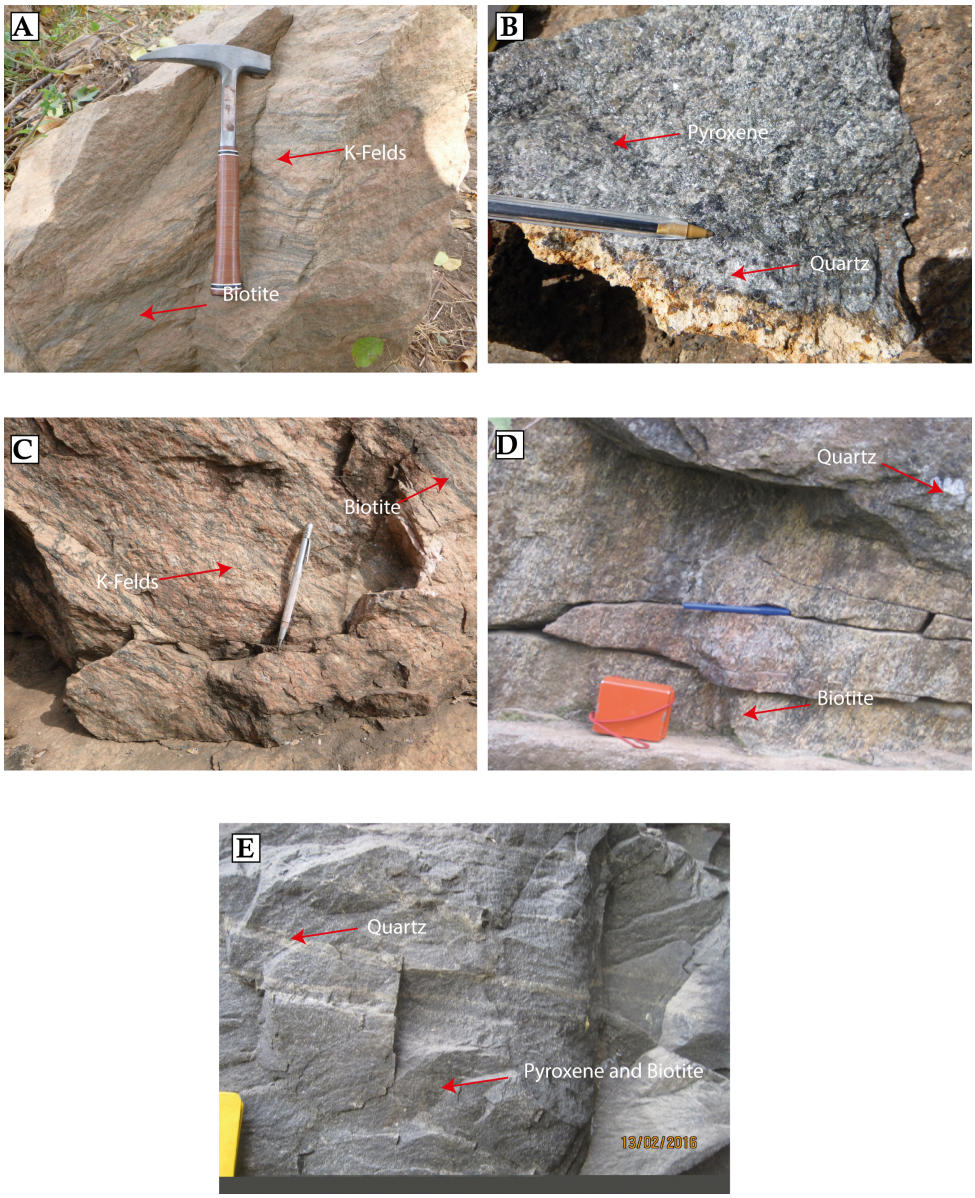

Figure 4. Macroscopic appearance (A, B, C, D, E) for samples.

4.5. Charnockitic Gneiss

Charnockitic gneiss (CIS 46) exhibits a rough foliation marked by dark streaks rich in ferromagnesian minerals such as biotite, orthopyroxene, and garnet. The rock is primarily composed of quartz and feldspar. Microscopically, it presents a

granoblastic structure with heterogeneous grain sizes. The quartz is xenomorphic, with low relief and rolling extinction, while larger quartz grains suggest metamorphic influence. Feldspar consists mainly of plagioclase with a few rare microcline crystals. The accessory phases include biotite, hypersthene, and opaque minerals (Figure 4(E)).

5. Whole Rock Geochemistry

The northern domain of the Man-Danané fault primarily consists of gray granulitic gneiss, charnockite, and pink granulite, with SiO_2 contents ranging from 68.6% to 73.4% and A/CNK ratios between 0.98 and 1.05.

In contrast, the southern domain of the fault comprises migmatitic biotite gneisses and hypersthene gneisses, displaying SiO_2 contents between 59.16% and 74.6%, with A/CNK ratios ranging from 0.81 to 1.03. These rock formations are generally weakly peraluminous, except for charnockite (CIS 26) and migmatitic biotite gneiss (CIS 44), which exhibit a metaluminous affinity (Figure 5).

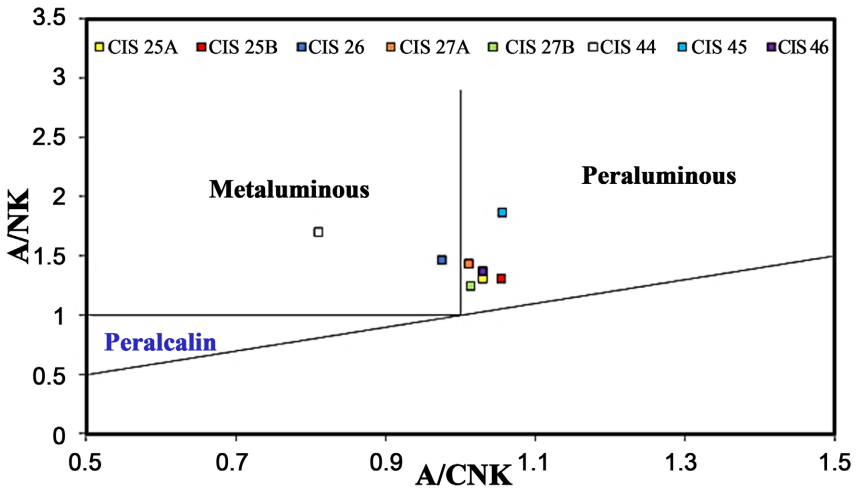

Figure 5. Shand diagram (1922) applied to all samples.

In the K_2O versus SiO_2 diagram of [33], CIS 25A, CIS 26, CIS 27A, and CIS 46 fall within the strongly potassic calc-alkaline series, CIS 25B and CIS 27B belong to the Shoshonitic series, CIS 44 aligns with the moderately potassic calc-alkaline series, CIS 45 follows a weakly potassic tholeiitic series (Figure 6).

The northern domain of the Man-Danané fault is mainly composed of gray granulitic gneiss, charnockite and pink granulite with SiO_2 contents ranging from 68.6% to 73.4%. The A/CNK ratios = 0.98 - 1.05. In addition, the petrographic study carried out in the domain south of this fault has revealed migmatitic biotite gneisses and hypersthene gneisses with SiO_2 contents ranging from 59.16% and 74.6% as well as A/CNK ratios = 0.81 - 1.03. All these rock formations are weakly peraluminous except for the Charnockite CIS 26 and the migmatitic biotite gneiss CIS 44 which have a metaluminous affinity (Figure 5). In the K_2O versus SiO_2 [33], CIS 25A, CIS 26 and CIS 27A, CIS 46 are located in the strongly potassic

calc-alkaline series, samples CIS 25B and CIS 27B are located in the shoshonitic series, CIS 44 in the moderately potassic calc-alkaline series and finally CIS 45 follows a tholeiitic series which is weakly potassic (**Figure 6**).

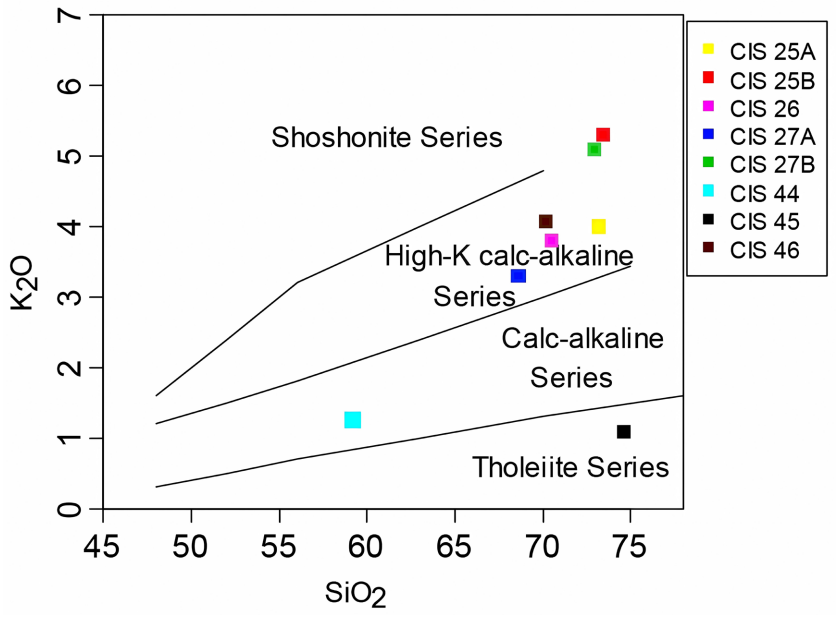

Figure 6. K_2O versus SiO_2 diagram from Pecerillo and Taylor (1976) applied to all samples.

The multi-element spectra of Biankouma and Kouibli samples, normalized to the primitive mantle (McDonough *et al.*, 1992) [34], exhibit a similar geochemical pattern. These rocks are notably enriched in large-ion lithophile elements (LILEs) such as Rb, Ba, and K, while showing depletions in high-field strength elements (HFSEs) like Nb, P, and Ti (**Figure 7**). Among them, CIS 27B displays a more pronounced depletion in heavy rare earth elements (HREEs). Additionally, the lithologies show a non-negligible enrichment in radioactive elements, particularly Th.

The observed Ba enrichment is likely linked to the granulitic metamorphic event responsible for their formation [35], suggesting that alkali feldspar fractionation over time was minimal. The negative anomalies in Ti, P, and Nb may indicate the presence of magnetite, sphene, apatite, and ilmenite in the melt residue or cumulate phases. Furthermore, the Ta-Nb depletion trend across all samples suggests that these granulitic gneisses originated from a subduction-related environment.

The total rare earth element content (ΣREE) varies from 107.7 ppm to 528.3 ppm. REE spectra, normalized to chondrites [34] (**Figure 8**), indicates a light rare earth element (LREE) enrichment, with (La/Sm) N ratios ranging from 7.99 to 8.45 and (La/Yb) N values spanning from 6.08 to 252.4. In contrast, there is a noticeable HREE depletion. Additionally, the granulitic gneisses exhibit a negative Eu anomaly (Eu/Eu = 0.39 - 1.67), indicative of plagioclase fractionation during fractional crystallization.

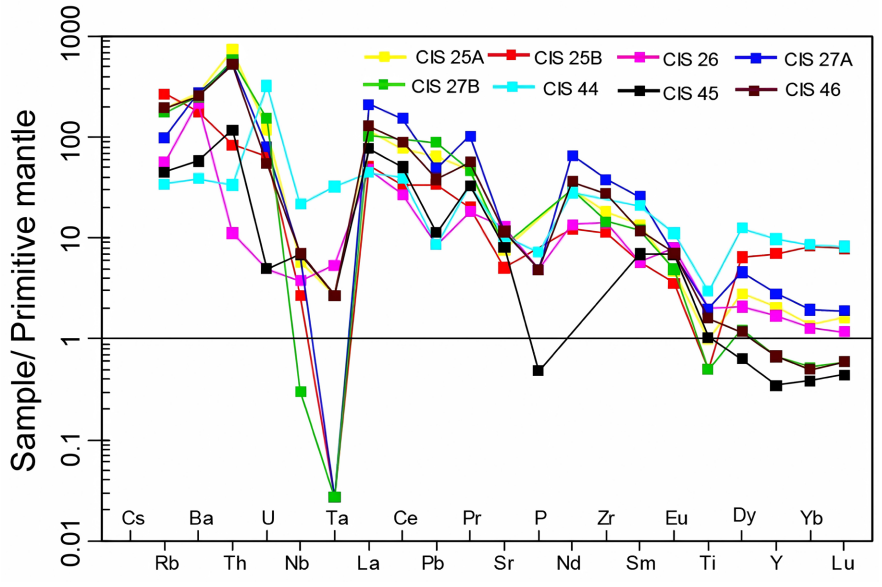

Figure 7. Primitive mantle-normalized multi-element spectra from McDonough *et al.* (1992).

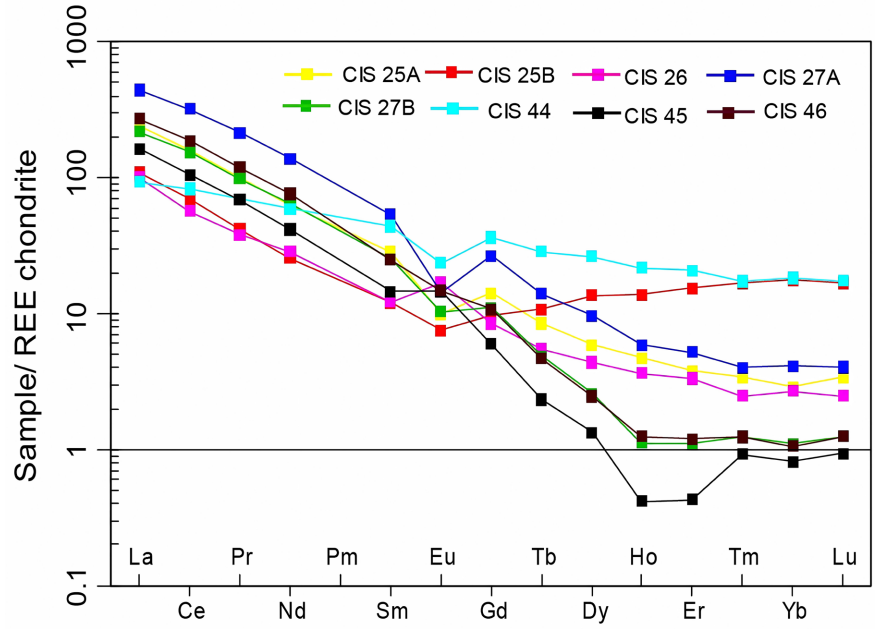

Figure 8. Chondrite-normalized rare earth spectra from Sun and McDonough (1992).

The multi-element spectra of the Biankouma and Kouibli samples normalized to the primitive mantle [34] show a similar pattern. These rocks are enriched in LILEs (Rb, Ba and K) and depleted in HFSE (Nb, P and Ti) (**Figure 7**). The depletion of heavy rare earths is more pronounced in the CIS 27B sample. The enrichment of these lithologies in radioactive elements (Th) is not negligible.

The enrichment in Ba could be due to the granulitic event that allowed the formation of these rocks [35] and would exclude a fractionation of the alkali feldspars over time. The negative anomalies in Ti, P and Nb could be assimilated to the

presence of magnetite, sphene, apatite and ilmenite in the melt residue or in the cumulate. The depression observed between Ta-Nb for all of these formations would indicate that these granulitic gneisses would come from a subduction environment.

The amount of rare earths (ΣREE) varies respectively from 107.7 ppm to 528.3 ppm. The rare earth spectra of the different rocks were normalized to the chondrites of [34] (**Figure 8**). These spectra are marked by an enrichment in light earths (LREE) with (La/Sm) N ratios that vary between 7.99 and 8.45; (La/Yb) N range from 6.08 to 252.4 and a depletion in heavy rare earths (HREE). Granulitic gneisses show a depletion in Eu (Eu/Eu* = 0.39 - 1.67). This depletion in Eu reflects a fractionation of plagioclase during fractional crystallization.

6. Discussion

6.1. Lithology

The petrographic study, based on macroscopic and microscopic analyses, has identified various metamorphic formations in the Biankouma and Kouibli regions, particularly north of the Man-Danané fault. These formations include granulitic gneisses, charnockite, and pink granulite in Biankouma, as well as migmatitic gneisses and charnockitic gneiss in Kouibli. The gray granulitic gneisses exhibit banding, a characteristic feature of Archean basement rocks [36]. [31] attributed this foliation to chemical variations from a basic to an acidic composition, with dioritic and tonalitic facies being the most dominant.

The granulitic gneiss has a granoblastic texture and is primarily composed of quartz and feldspar with hypersthene, while garnet is present as an accessory mineral. Similar lithologies have been described in the granulitic domain of the Man region by [30] [31], and [13]. Although granodiorite was not observed in this study, the lithological findings align with those of [30], who described the northern granulite domain of Man as comprising gray granulitic gneisses, Mangouin charnockite, pink granulite, and granodiorite.

Additionally, gneisses, granulites, and charnockites have been documented in the Yacouba complex [32], though a clear distinction between charnockite and granulite was not made. The mineralogical association of quartz, hypersthene, plagioclase (perthite), and garnet suggests that these formations underwent high-grade metamorphism in the granulite facies. In Kouibli, biotite migmatitic gneisses and charnockitic gneiss were also identified, consistent with the findings of [14].

The petrographic study allowed, by a macroscopic and microscopic approach, to highlight metamorphic formations namely granulitic gneisses, charnockite, pink granulite in the Biankouma region, migmatitic gneisses and charnockitic gneiss in the Kouibli area like all the regions located north of Man-Danané fault. The gray granulitic gneisses show a banding which is a primary magmatic character in the old Archean basements [36]. These foliations are described by [31] as the variation of chemistry going from a basic pole to an acid pole. The dioritic and tonalitic facies are the most abundant. The granulitic gneiss has a granoblastic

texture. It is an essentially quartzo-feldspathic rock with hypersthene. The accessory phase of these granulitic gneisses is composed of garnet. This type of formation was observed and described by [30] [31] and [13] in the granulitic domain of the Man region. Except for granodiorite which was not observed in this study, the lithologies encountered in the study area support the results obtained in the northern granulite domain of the Man region by [30]. Indeed, this author describes this domain as consisting essentially of granulitic gray gneisses associated with Mangouin charnockite, pink granulite and granodiorite. The gneisses, granulite and charnockite were described by [32] within the Yacouba complex without however making the difference between charnockite and granulite. The mineralogical association (quartz, hypersthene, plagioclase (perthite) and garnet) of these different formations indicates that they have undergone high-grade metamorphism in the granulite facies. In the Kouibli area, biotite migmatitic gneisses and charnockitic gneiss have been observed [14].

6.2. Geochemical Evolution and Geotectonic Environments

The geochemical analysis of formations from Biankouma to Kouibli reveals that these rocks belong to the tonalite-trondhjemite-granodiorite (TTG) suite), with variable compositions. According to the An-Ab-Or diagram [37], these formations are predominantly granodioritic, although some granitic and tonalitic occurrences (**Figure 9**) are also present. However, they differ from the TTGs studied by [38] in Finland, India, and Brazil.

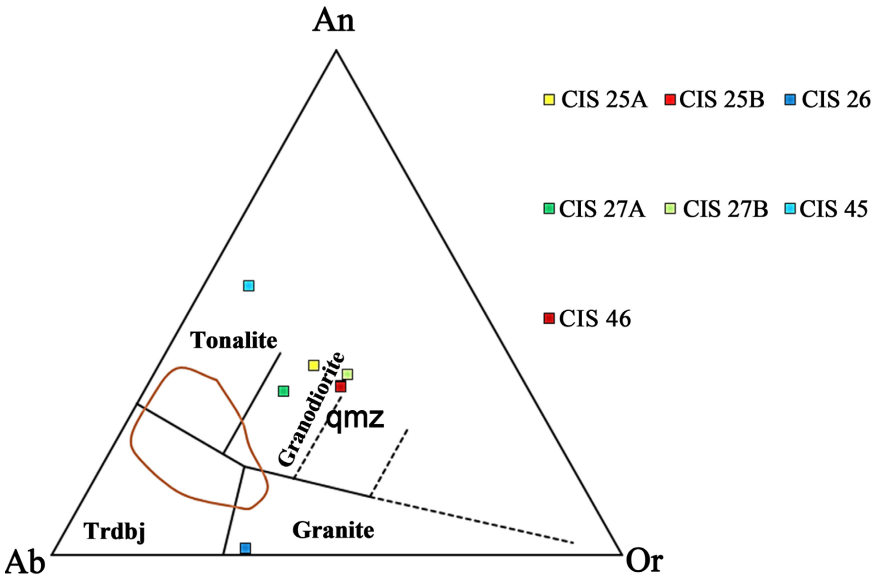

Figure 9. Barker's (1979) An-Ab-Or diagram applied to all samples. The circled area represents the samples studied by Martin (1994) [38]. Martin: TTG from Finland, India, and Brazil.

Based on alumina content, TTGs are classified into two types [37] [39] Al-rich TTGs ($Al_2O_3 > 15\%$), Al-poor TTGs ($Al_2O_3 < 15\%$).

With Al_2O_3 contents ranging from 13.09% to 14.81%, the Archean rocks of Man belong to the Al-poor TTG category. Their geochemical signatures indicate a weakly peraluminous to strongly metaluminous nature. According to [40], the metaluminous affinity suggests a mantle origin, implying that these formations may have derived from mantle sources. Conversely, the peraluminous nature of charnockite (CIS 26) and migmatitic gneiss (CIS 44) suggests a crustal origin [40].

Furthermore, the studied formations exhibit subalkaline to alkaline characteristics, predominantly following a strongly calc-alkaline lineage. These findings align with [31], who demonstrated, using the Q-Ab-Or diagram [37], that the banded gneisses of the northern domain follow a calc-alkaline trend.

6.3. Geochemical Anomalies and Tectonic Implications

All the studied formations exhibit negative anomalies in Nb, Ti, and P, with Th showing a weaker anomaly. The depletion of Ti, Nb, and P suggests the presence of ilmenite and apatite in the residual melt or cumulate phase [30]. In the case of pink granulite, the Th anomaly is attributed to granulitic metamorphism during its emplacement. Similar formations with negative Th anomalies have been identified in the Scourie complex in Scotland, where they are classified as leucogneisses. [41] proposes that acid leucogneisses result from the partial melting of tonalite during the prograde phase of granulitic metamorphism.

The genesis of TTG (tonalite-trondhjemite-granodiorite) suites has been a long-standing topic of debate. There are two main hypotheses:

1) Fractional crystallization of a hydrated basaltic liquid [39] [42].

2) Partial melting of a basic source rock, such as an amphibolite [43]-[45].

With the exception of pink granulite (CIS25B), which exhibits a high YbN content and a low LaN/YbN ratio, the TTGs in the Archean Man domain display YbN values between 0.82 and 4.13, and LaN/YbN ratios from 36.79 to 252.42. These characteristics classify them as Archean TTGs. According to Martin (1993) [46], Archean TTGs are distinguished by low YbN values (<8.5) and high LaN/YbN ratios, unlike post-Archean TTGs.

6.4. Subduction Environment and Magmatic Processes

The studied samples are positioned within the volcanic arc field (**Figure 10**). The observed negative europium (Eu) anomalies indicate the fractionation of plagioclase in the melt, while the depletion in heavy rare earth elements (HREEs) suggests the presence of garnet in the residual liquid. Additionally, the negative Ta-Nb anomalies across all samples further support a subduction-related origin.

From these findings, the most plausible hypothesis for the formation of Archean TTGs in the Man domain is their derivation from the partial melting of a basic source, specifically an amphibolite containing garnet and hornblende [39] [43] [47]. This process is believed to occur in a subduction zone [48] [49].

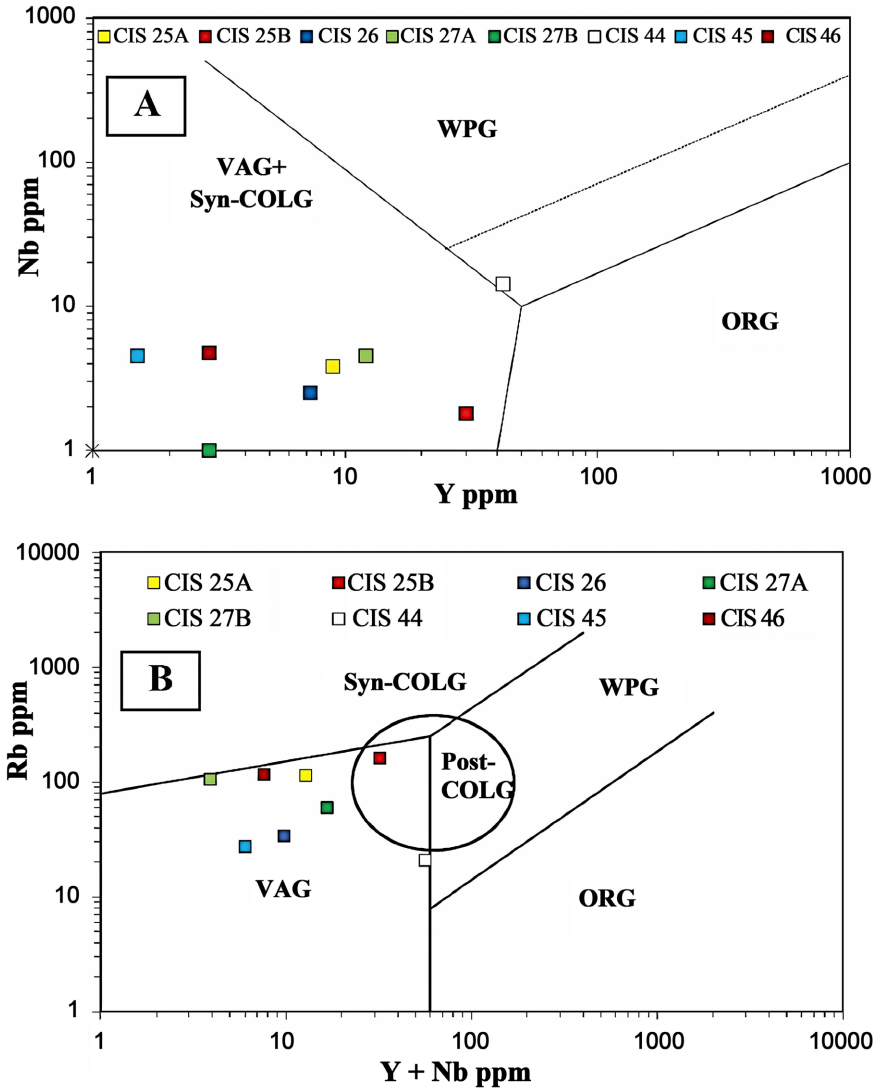

Figure 10. Position of samples in the geotectonic diagrams of [50]. Nb vs. Y; (B) Rb vs. (Yb + Ta). VAG = volcanic arc granites; WPG = intraplate anorogenic domain-related granites; ORG = oceanic ridge granites; Syn-COLG = syncollisional; Post-COLG: Postcollisional.

7. Conclusion

The aim of this study was to characterize the gneissic formations of the Biankouma and Kouibli areas, investigate their geochemical properties, and propose a model for their emplacement. From a petrographic perspective, the Archean domain of the Biankouma area extending into the Kouibli area is primarily composed of granulitic gneiss, charnockites, and pink granulite in Biankouma, with biotite migmatite gneiss and charnockitic gneiss in Kouibli. The mineralogy of these metamorphic formations includes quartz, alkali feldspar, hypersthene, plagioclase, and biotite, all formed under granulite facies conditions. Geochemical analysis reveals that the studied formations are Archean TTGs with granodioritic, tonalitic, and granitic compositions. These rocks are characterized by low aluminum content (Al_2O_3 < 15%) and exhibit a strongly potassic to tholeiitic calc-alkaline affinity. The for-

mations display a weakly metaluminous to weakly peraluminous nature. Trace element distributions show enrichments in light rare earth elements (LREEs) and depletions in heavy rare earth elements (HREEs). The negative anomalies in Ta-Nb and Eu further support the hypothesis that these formations originated from the partial melting of a basic source rock containing garnet and hornblende. The composition of all samples suggests an arc and collision granite signature, consistent with their formation in a subduction zone.

Acknowledgements

The analyses and fieldwork were financially supported by PRESED-CI T2GEM research grant "Geophysical and Geochemical Techniques for Mining Exploration". We would like to thank the PASRES (Strategic Support Program for Scientific Research) for contributions to the field campaign.

Conflicts of Interest

The authors declare no conflicts of interest regarding the publication of this paper.

References

[1] Rudnick, R.L. (1995) Making Continental Crust. *Nature*, **378**, 571-578. https://doi.org/10.1038/378571a0

[2] Dhuime, B., Hawkesworth, C.J., Cawood, P.A. and Storey, C.D. (2012) A Change in the Geodynamics of Continental Growth 3 Billion Years Ago. *Science*, **335**, 1334-1336. https://doi.org/10.1126/science.1216066

[3] Fisher, C.M. and Vervoort, J.D. (2018) Using the Magmatic Record to Constrain the Growth of Continental Crust—The Eoarchean Zircon Hf Record of Greenland. *Earth and Planetary Science Letters*, **488**, 79-91. https://doi.org/10.1016/j.epsl.2018.01.031

[4] Mareschal, J. and Jaupart, C. (2006) Archean Thermal Regime and Stabilization of the Cratons. In: Benn, K., Mareschal, J.-C. and Condie, K.C., Eds., *Archean Geodynamics and Environments*, American Geophysical Union, 61-73. https://doi.org/10.1029/164gm06

[5] Savanier, D., Guille, G., Maury, R.C., Blais, S., Guillou, H., Legendre C., *et al.* (2003) Geology, Petrology and Radiochronology of Nuku Hiva (Marquesas Island, French Polynesia). *EGS-AGU-EUG Joint Assembly*, Nice, 6-11 April 2003, 6-11.

[6] Kouamelan, A.N., Delor, C. and Peucat, J. (1997) Geochronological Evidence for Reworking of Archean Terrains during the Early Proterozoic (2.1 Ga) in the Western Côte d'Ivoire (Man Rise-West African Craton). *Precambrian Research*, **86**, 177-199. https://doi.org/10.1016/s0301-9268(97)00043-0

[7] François, C., Philippot, P. and Rey, P. (2012) Formation and Exhumation Mechanisms of High-Grade Rocks: Sagduction and Subduction Processes during the Archean. *Geophysical Research Abstracts*, **14**, EGU2012-5136.

[8] Lin, S., Parks, J., Heaman, L.M., Simonetti, A. and Corkery, M.T. (2013) Diapirism and Sagduction as a Mechanism for Deposition and Burial of "Timiskaming-Type" Sedimentary Sequences, Superior Province: Evidence from Detrital Zircon Geochronology and Implications for the Borden Lake Conglomerate in the Exposed Middle to Lower Crust in the Kapuskasing Uplift. *Precambrian Research*, **238**, 148-157. https://doi.org/10.1016/j.precamres.2013.09.012

[9] François, C., Philippot, P., Rey, P. and Rubatto, D. (2014) Burial and Exhumation during Archean Sagduction in the East Pilbara Granite-Greenstone Terrane. *Earth and Planetary Science Letters*, **396**, 235-251. https://doi.org/10.1016/j.epsl.2014.04.025

[10] Johnson, T.E., Brown, M., Goodenough, K.M., Clark, C., Kinny, P.D. and White, R.W. (2016) Subduction or Sagduction? Ambiguity in Constraining the Origin of Ultramafic-Mafic Bodies in the Archean Crust of NW Scotland. *Precambrian Research*, **283**, 89-105. https://doi.org/10.1016/j.precamres.2016.07.013

[11] Canfield, D.E. (2005) The Early History of Atmospheric Oxygen: Homage to Robert M. Garrels. *Annual Review of Earth and Planetary Sciences*, **33**, 1-36. https://doi.org/10.1146/annurev.earth.33.092203.122711

[12] Hou, K., Li, Y. and Wan, D. (2007) Constraints on the Archean Atmospheric Oxygen and Sulfur Cycle from Mass-Independent Sulfur Records from Anshan-Benxi BIFs, Liaoning Province, China. *Science in China Series D*: *Earth Sciences*, **50**, 1471-1478. https://doi.org/10.1007/s11430-007-0106-9

[13] Koffi, G.R., Kouamelan, A.N., Allialy, M.E., Coulibaly, Y. and Peucat, J. (2020) Re-evaluation of Leonian and Liberian Events in the Geodynamical Evolution of the Man-Leo Shield (West African Craton). *Precambrian Research*, **338**, Article 105582. https://doi.org/10.1016/j.precamres.2019.105582

[14] Pitra, P., Kouamelan, A.N., Ballèvre, M. and Peucat, J. (2010) Palaeoproterozoic High-pressure Granulite Overprint of the Archean Continental Crust: Evidence for Homogeneous Crustal Thickening (Man Rise, Ivory Coast). *Journal of Metamorphic Geology*, **28**, 41-58. https://doi.org/10.1111/j.1525-1314.2009.00852.x

[15] Baratoux, L., Metelka, V., Naba, S., Jessell, M.W., Grégoire, M. and Ganne, J. (2011) Juvenile Paleoproterozoic Crust Evolution during the Eburnean Orogeny (~2.2 - 2.0 Ga), Western Burkina Faso. *Precambrian Research*, **191**, 18-45. https://doi.org/10.1016/j.precamres.2011.08.010

[16] Milési, J.-P., Feybesse, J.-L. and Pinna, P. (2004) Geological Map of Africa 1:10,000,000, SIG Afrique Project. 20*th Conference of African Geology*, Orléans, 2-7 June 2004.

[17] Thiéblemont, D., Goujou, J.C., Egal, E., Cocherie, A., Delor, C., Lafon, J.M., *et al.* (2004) Archean Evolution of the Leo Rise and Its Eburnean Reworking. *Journal of African Earth Sciences*, **39**, 97-104. https://doi.org/10.1016/j.jafrearsci.2004.07.059

[18] Kouamelan, A.N., Peucat, J.J. and Delor, C. (1997) Reliques archéennes (3.15 Ga) au sein du magmatisme Birimien (2.1 Ga) de C6te d'Ivoire, Craton Ouest-Africain. *Comptes rendus de l'Académie des Sciences*, 324, 719-727.

[19] Allibone, A.H., McCuaig, T.C., Harris, D., Etheridge, M., Munroe, S., Byrne, D., *et al.* (2002) Structural Controls on Gold Mineralization at the Ashanti Deposit, Obuasi, Ghana. In: Goldfarb, R.J. and Nielsen, R.L., Eds., *Integrated Methods for Discovery-Global Exploration in the Twenty-First Century*, Society of Economic Geologists, 65-94. https://doi.org/10.5382/sp.09.04

[20] Feybesse, J., Billa, M., Guerrot, C., Duguey, E., Lescuyer, J., Milesi, J., *et al.* (2006) The Paleoproterozoic Ghanaian Province: Geodynamic Model and Ore Controls, Including Regional Stress Modeling. *Precambrian Research*, **149**, 149-196. https://doi.org/10.1016/j.precamres.2006.06.003

[21] Pouclet, A., Doumbia, S. and Vidal, M. (2006) Geodynamic Setting of the Birimian Volcanism in Central Ivory Coast (Western Africa) and Its Place in the Palaeoproterozoic Evolution of the Man Shield. *Bulletin de la Société Géologique de France*, **177**, 105-121. https://doi.org/10.2113/gssgfbull.177.2.105

[22] Tshibubudze, A., Hein, K.A.A. and Marquis, P. (2009) The Markoye Shear Zone in

NE Burkina Faso. *Journal of African Earth Sciences*, **55**, 245-256. https://doi.org/10.1016/j.jafrearsci.2009.04.009

[23] Wane, O., Liégeois, J., Thébaud, N., Miller, J., Metelka, V. and Jessell, M. (2018) The Onset of the Eburnean Collision with the Kenema-Man Craton Evidenced by Plutonic and Volcanosedimentary Rock Record of the Masssigui Region, Southern Mali. *Precambrian Research*, **305**, 444-478. https://doi.org/10.1016/j.precamres.2017.11.008

[24] Grenholm, M., Jessell, M. and Thébaud, N. (2019) Paleoproterozoic Volcano-Sedimentary Series in the Ca. 2.27 - 1.96 Ga Birimian Orogen of the Southeastern West African Craton. *Precambrian Research*, **328**, 161-192. https://doi.org/10.1016/j.precamres.2019.04.005

[25] Grenholm, M., Jessell, M. and Thébaud, N. (2019) A Geodynamic Model for the Paleoproterozoic (ca. 2.27 - 1.96 Ga) Birimian Orogen of the Southern West African Craton—Insights into an Evolving Accretionary-Collisional Orogenic System. *Earth-Science Reviews*, **192**, 138-193. https://doi.org/10.1016/j.earscirev.2019.02.006

[26] McFarlane, H.B., Thébaud, N., Parra-Avila, L.A., Armit, R., Spencer, C., Ganne, J., *et al.* (2019) Onset of the Supercontinent Cycle: Evidence for Multiple Oceanic Arc Accretion Events in the Paleoproterozoic Sefwi Greenstone Belt of the West African Craton. *Precambrian Research*, **335**, Article 105450. https://doi.org/10.1016/j.precamres.2019.105450

[27] Hirdes, W. and Davis, D.W. (2002) U-Pb Geochronology of Paleoproterozoic Rocks in the Southern Part of the Kedougou-Kéniéba Inlier, Senegal, West Africa: Evidence for Diachronous Accretionary Development of the Eburnean Province. *Precambrian Research*, **118**, 83-99. https://doi.org/10.1016/s0301-9268(02)00080-3

[28] Gasquet, D., Barbey, P., Adou, M. and Paquette, J.L. (2003) Structure, Sr-Nd Isotope Geochemistry and Zircon U-Pb Geochronology of the Granitoids of the Dabakala Area (Côte d'Ivoire): Evidence for a 2.3 Ga Crustal Growth Event in the Palaeoproterozoic of West Africa? *Precambrian Research*, **127**, 329-354. https://doi.org/10.1016/s0301-9268(03)00209-2

[29] Mériaud, N., Thébaud, N., Masurel, Q., Hayman, P., Jessell, M., Kemp, A., *et al.* (2020) Lithostratigraphic Evolution of the Bandamian Volcanic Cycle in Central Côte d'Ivoire: Insights into the Late Eburnean Magmatic Resurgence and Its Geodynamic Implications. *Precambrian Research*, **347**, Article 105847. https://doi.org/10.1016/j.precamres.2020.105847

[30] Kouamelan, A.N. (1996) Géochronologie et Géochimie des formations archéennes et protérozoïques de la dorsale de Man en Côte d'Ivoire: Implication pour la transition Archéen Protérozoïque. Mémoire Géosciences Rennes n˚73.

[31] Camil J. (1984) Pétrographie, chronologie des ensembles granulitiques archéens et formations associées de la région de Man (Côte d'Ivoire). Implications pour l'histoire géologique du craton Ouest Africain. Thèse Doctor, Université d'Abidjan.

[32] Gouedji, F., Picard, C., Coulibaly, Y., Audet, M., Auge, T., Goncalves, P., *et al.* (2014) The Samapleu Mafic-Ultramafic Intrusion and Its Ni-Cu-PGE Mineralization: An Eburnean (2.09 Ga) Feeder Dyke to the Yacouba Layered Complex (Man Archean Craton, Western Ivory Coast). *Bulletin de la Société Géologique de France*, **185**, 393-411. https://doi.org/10.2113/gssgfbull.185.6.393

[33] Peccerillo, A. and Taylor, S.R. (1976) Geochemistry of Eocene Calc-Alkaline Volcanic Rocks from the Kastamonu Area, Northern Turkey. *Contributions to Mineralogy and Petrology*, **58**, 63-81. https://doi.org/10.1007/bf00384745

[34] McDonough, W.F., Sun, S.-S., Ringwood, A.E., Jagoutz, E. and Hofmann, A.W.

(1992) Potassium, Rubidium, and Cesium in the Earth and Moon and the Evolution of the Mantle of the Earth. *Geochimica et Cosmochimica Acta*, **56**, 1001-1012. https://doi.org/10.1016/0016-7037(92)90043-i

[35] Barbey, P. and Cuney, M. (1982) K, Rb, Sr, Ba, U and Th Geochemistry of the Lapland Granulites (Fennoscandia). LILE Fractionation Controlling Factors. *Contributions to Mineralogy and Petrology*, **81**, 304-316. https://doi.org/10.1007/bf00371685

[36] Coolen, J.J.M.M.M. (1980) Chemical Petrology of the Furua Granulite Complex, Southern Tanzania. GUA.

[37] Barker, F. (1979) Trondhjemite: Definition, Environment and Hypotheses of Origin. *Developments in Petrology*, **6**, 1-12. https://doi.org/10.1016/b978-0-444-41765-7.50006-x

[38] Martin, H. (1994) Chapter 6 the Archean Grey Gneisses and the Genesis of Continental Crust. *Developments in Precambrian Geology*, **11**, 205-259. https://doi.org/10.1016/s0166-2635(08)70224-x

[39] Barker, F. and Arth, J.G. (1976) Generation of Trondhjemitic-Tonalitic Liquids and Archean Bimodal Trondhjemite-Basalt Suites. *Geology*, **4**, 596-600. https://doi.org/10.1130/0091-7613(1976)4<596:gotlaa>2.0.co;2

[40] Debon, F. and Le Fort, P. (1988) A Cationic Classification of Common Plutonic Rocks and Their Magmatic Associations: Principles, Method, Applications. *Bulletin de Minéralogie*, **111**, 493-510. https://doi.org/10.3406/bulmi.1988.8096

[41] Cartwright, I. (1990) Prograde Metamorphism, Anatexis, and Retrogression of the Scourian Complex, North-West Scotland. In: Ashworth, J.R. and Brown, M., Eds., *High-Temperature Metamorphism and Crustal Anatexis*, Springer, 371-399. https://doi.org/10.1007/978-94-015-3929-6_13

[42] Arth, J.G., Barker, F., Peterman, Z.E. and Friedman, I. (1978) Geochemistry of the Gabbro-Diorite-Tonalite-Trondhjemite Suite of Southwest Finland and Its Implications for the Origin of Tonalitic and Trondhjemitic Magmas. *Journal of Petrology*, **19**, 289-316. https://doi.org/10.1093/petrology/19.2.289

[43] Arth, J.G. and Hanson, G.N. (1975) Geochemistry and Origin of the Early Precambrian Crust of Northeastern Minnesota. *Geochimica et Cosmochimica Acta*, **39**, 325-362. https://doi.org/10.1016/0016-7037(75)90200-8

[44] Martin, H. (1986) Effect of Steeper Archean Geothermal Gradient on Geochemistry of Subduction-Zone Magmas. *Geology*, **14**, 753-756. https://doi.org/10.1130/0091-7613(1986)14<753:eosagg>2.0.co;2

[45] MARTIN, H. (1987) Petrogenesis of Archaean Trondhjemites, Tonalites, and Granodiorites from Eastern Finland: Major and Trace Element Geochemistry. *Journal of Petrology*, **28**, 921-953. https://doi.org/10.1093/petrology/28.5.921

[46] Martin, H. (1993) The Mechanisms of Petrogenesis of the Archaean Continental Crust—Comparison with Modern Processes. *Lithos*, **30**, 373-388. https://doi.org/10.1016/0024-4937(93)90046-f

[47] Drummond, M.S. and Defant, M.J. (1990) A Model for Trondhjemite-Tonalite-Dacite Genesis and Crustal Growth via Slab Melting: Archean to Modern Comparisons. *Journal of Geophysical Research*: *Solid Earth*, **95**, 21503-21521. https://doi.org/10.1029/jb095ib13p21503

[48] Foley, S., Tiepolo, M. and Vannucci, R. (2002) Growth of Early Continental Crust Controlled by Melting of Amphibolite in Subduction Zones. *Nature*, **417**, 837-840. https://doi.org/10.1038/nature00799

[49] Martin, H., Moyen, J., Guitreau, M., Blichert-Toft, J. and Le Pennec, J. (2014) Why

Archaean TTG Cannot Be Generated by MORB Melting in Subduction Zones. *Lithos*, **198**, 1-13. https://doi.org/10.1016/j.lithos.2014.02.017

[50] Pearce, J.A., Harris, N.B.W. and Tindle, A.G. (1984) Trace Element Discrimination Diagrams for the Tectonic Interpretation of Granitic Rocks. *Journal of Petrology*, **25**, 956-983. https://doi.org/10.1093/petrology/25.4.956